

HEAT TRANSFER PROCESS IN A HOT DRY ROCK GEOTHERMAL RESERVOIR

Shinji Yamaguchi and Satoshi Akibayashi

Department of Mining Engineering, Akita University, Akita, Japan

SUMMARY - The authors developed a numerical model which could simulate thermal energy transport in rock matrix/fracture network system constituting hot dry rock geothermal reservoir. Some sensitivity studies were performed with the numerical model and following results were obtained: (1) Water injection rate has a large influence on the bottom hole temperature of the production well, (2) matrix rock conductivity controls the heat transfer from matrix rock to the fluid in fractures, (3) drilling mud invasion during the production well drilling influences the length of hot water production time, (4) the length of connected fractures affects the bottom hole temperature of the production well.

1. INTRODUCTION

Since 1985, a research and development on the technique of heat extraction from hot dry rock has been performed by NEDO (New Energy and Industrial Technology Development Organization) at Hijiori, Yamagata prefecture, Japan (NEDO, 1991). Heat extraction tests showed injected water reached the production well through existing and artificially created fractures. Therefore, heat transfer process between hot dry rock and water through fractures connected each other should be investigated to evaluate heat recovery from hot dry rock geothermal reservoir.

Several works have been done for modeling on fluid and heat flow in the area of fractured rock (Chida et al., 1990; Gringarten et al., 1975; Kimura et al., 1991; Masuda et al., 1991; Pruess, 1985). Because previous models were developed to analyze fluid and heat flow in the rock mass with a single fracture or some parallel fractures, it is difficult to apply them to the matrix rock/fracture network system

which might constitute hot dry rock geothermal reservoir as shown in Fig.1. The authors developed a numerical model which could simulate thermal energy transport in matrix rock/fracture network system mentioned above (Akibayashi et al., 1992).

This paper introduces the numerical model briefly and discusses the following effects on the heat transfer phenomena between injected water and matrix rock: the effect of water injection rate, thermal conductivity of matrix rock, drilling mud invasion, and connected fracture length.

2. MATHEMATICAL MODEL

The mathematical model used in this paper is described precisely in the published paper (Akibayashi et al., 1992). Therefore this chapter just summarizes the model briefly.

Fig.2 shows an idealized horizontal model of the artificial reservoir system which consists of connected fractures and matrix blocks of Fig.1.

2.1 Major Assumptions

Major assumptions made in this study are as follows.

- 1) The artificial reservoir consists of matrix blocks and fracture networks as shown in Fig.1.
- 2) Within fractures, (a) fluid flow is in one-dimensional steady state and obeys the Darcy's law, (b) fluid storage capacity is very small, (c) heat transfer is in two-dimensional unsteady state and controlled by both hydrodynamic dispersion and advection, (d) fractures are filled with homogeneous solids and (e) thermal equilibrium between fluid and solid is reached instantaneously.
- 3) Within matrix blocks, (a) no permeability and fluid storage capacity are assumed, (b) heat transfer is dominated

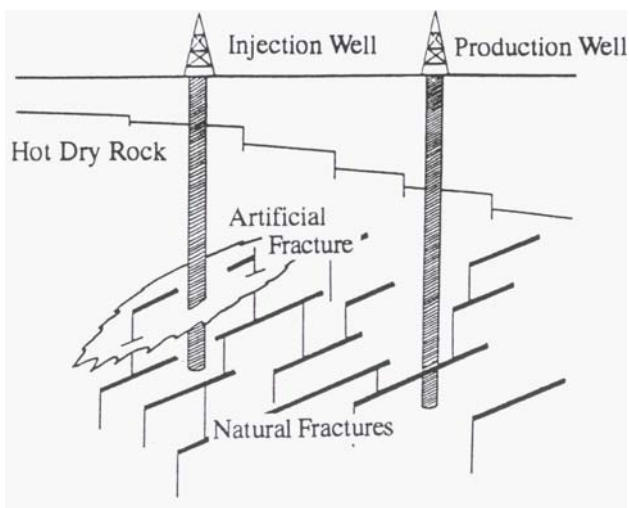


Figure 1-Concept of an artificial reservoir in a hot dry rock

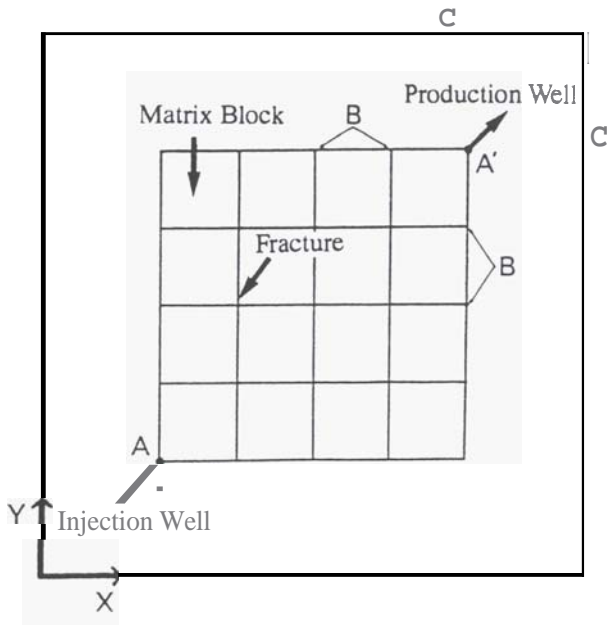


Figure 2- An idealized horizontal model of an artificial reservoir

by heat conduction and is in two-dimensional unsteady state.

4) Between matrix blocks and fractures, (a) heat exchange is governed by the Fourier's conduction law, (b) no resistance to heat transfer is assumed at the interfaces.

2.2 Governing Equations

Based on the above assumptions, the basic equations governing fluid flow in fractures and energy transport in fractures and matrix blocks can be written in the following forms.

An equation for fluid flow through fractures- In the case where fractures are completely filled with homogeneous solids, the flow relationship for laminar flow simply becomes the Darcy's law.

$$q = \frac{C(2b)WK\nabla\Phi}{\mu} \quad (1)$$

Where

q = flow rate, m^3/day

C = unit conversion factor

$2b$ = aperture of a fracture, m

W = fracture width, m

K = permeability, m^2

Φ = potential, Pa

μ = viscosity, $Pa \cdot s$

Equations for energy transport in fractures-

$$\nabla \cdot (\lambda_f \nabla \theta_f) - c_f \rho_f V \nabla \theta_f + E_c + E_d + E_{in} = \frac{\partial}{\partial t} \quad (2)$$

where

$$c_e \rho_e = c_f \rho_f \phi_f + c_s \rho_s (1 - \phi_f) \quad (3)$$

$$\lambda_f = \lambda_e + 0.5 D_p \phi_f c_f \rho_f V \quad (\text{Wakao, et al., 1979}) \quad (4)$$

λ_f = thermal conductivity of fracture, $Kcal/m \cdot day \cdot ^\circ C$

θ_f = fracture temperature, $^\circ C$

c_f = specific heat of liquid, $Kcal/kg \cdot ^\circ C$

ρ_f = liquid density, kg/m^3

V = liquid velocity, m/day

E_c = energy flux due to advection, $Kcal/m^3 \cdot day$

E_d = energy flux due to conduction, $Kcal/m^3 \cdot day$

E_{in} = energy flux due to injection, $Kcal/m^3 \cdot day$

c_e = effective specific heat, $Kcal/kg \cdot ^\circ C$

ρ_e = effective density, kg/m^3

t = time, day

ϕ_f = fracture porosity

c_s = specific heat of solid, $Kcal/kg \cdot ^\circ C$

ρ_s = solid density, kg/m^3

λ_e = effective thermal conductivity, $Kcal/m \cdot day \cdot ^\circ C$

D_p = particle diameter, m

E_c and E_d terms in Eq.(2) are defined as follows, respectively:

For x-directional fractures,

$$E_c = -c_f \rho_f V_y \nabla_y \theta_f \quad (5)$$

$$E_d = -\frac{1}{2b} (\lambda_m \nabla_y \theta_m, Y=-b + \lambda_m \nabla_y \theta_m, Y=b) \quad (6)$$

where

$$\nabla_y = \frac{\partial}{\partial Y} \quad (7)$$

V_y = liquid velocity in y-direction, m/day

λ_m = thermal conductivity of matrix, $Kcal/m \cdot day \cdot ^\circ C$

θ_m = matrix temperature, $^\circ C$

$Y = Y$ components in Cartesian coordinate

For y-directional fractures.

$$E_c = -c_f \rho_f V_x \nabla_x \theta_f \quad (8)$$

$$E_d = -\frac{1}{2b} (\lambda_m \nabla_x \theta_m, X=-b + \lambda_m \nabla_x \theta_m, X=b) \quad (9)$$

Where

$$\nabla_x = \frac{\partial}{\partial X} \quad (10)$$

V_x = liquid velocity in x-direction, m/day

$X = X$ components in Cartesian coordinate

The solution of Eq.(2) is obtained under following initial

and boundary conditions:

$$\theta_f = \theta_{\max} \quad \text{at } t = 0 \quad (11)$$

$$\theta_m = \theta_{\max} \quad (12)$$

$$\theta_f = \theta_o \quad \text{at the injection well} \quad (13)$$

(Point A in Fig.2)

$$E_{in} = 0 \quad (14)$$

$$\nabla \theta_f = 0 \quad \text{at the fracture flow boundary} \quad (15)$$

(Boundary B in Fig.2)

where

$$\theta_{\max} = \text{maximum temperature, } ^\circ\text{C}$$

$$\theta_o = \text{initial temperature, } ^\circ\text{C}$$

Equations for energy transport in matrix blocks-

$$\nabla \cdot (\lambda_m \nabla \theta_m) - E_d = c_m \rho_m \frac{\partial \theta_m}{\partial t} \quad (16)$$

Where

$$c_m = \text{specific heat of matrix, Kcal/kg} \cdot ^\circ\text{C}$$

$$\rho_m = \text{matrix density, kg/m}^3$$

The solution of Eq.(10) is obtained under following initial and boundary conditions:

$$\theta_m = \theta_{\max} \quad \text{at } t = 0 \quad (17)$$

$$\nabla \theta_m = 0 \quad \text{at outer boundary} \quad (18)$$

(Boundary C in Fig.2)

2.3 Solution Methods

System of equations for fluid flow in fractures- Because of the assumption that fluid flow in fractures is in steady state, fluid volume flowing through each fracture can be obtained by applying the continuity equation at each node in the fracture system.

$$\sum_{i=1}^n q_i = 0 \quad (19)$$

where

$$n = \text{number of fractures intersecting a given node}$$

$$I = \text{X-coordinate of fracture}$$

The sign of q is defined as positive if the liquid is entering the node and negative if it is leaving. The resulting linear system of equations can be solved by use of the elimination method for a banded matrix. The boundary conditions are as follows:

$$q = q_{in} \quad \text{at the injection well} \quad (20)$$

(Point A in Fig.2)

$$q = q_{out} \quad \text{at the production well} \quad (21)$$

(Point A in Fig.2)

where

$$q_{in} = \text{injection flow rate, m}^3/\text{day}$$

$$q_{out} = \text{production flow rate, m}^3/\text{day}$$

Equations for energy transport in fractures- Eqs.(2) through (15) were approximated by finite difference equations, resulting in a system of equations. The system of equations was solved with Alternating Direction Implicit procedure by assuming source terms E_i and E_d were known from the previous time.

Equations for energy transport in matrix blocks- Eqs.(16) through (18) were approximated by finite difference equations, resulting in a system of equations. The system of equations was solved with Peaceman and Rachford's ADI procedure by assuming the source term E_i was known from the previous time.

3. SENSITIVITY STUDIES AND DISCUSSION

The effects of the following four variables on the bottom hole temperature of the production well were discussed. The variables were (1) water injection rate, (2) thermal conductivity of the matrix rock, (3) drilling mud invasion, (4) connected fracture length. Figd shows the flow path of injected water through fractures and Table 1 lists major input data used in the following calculations.

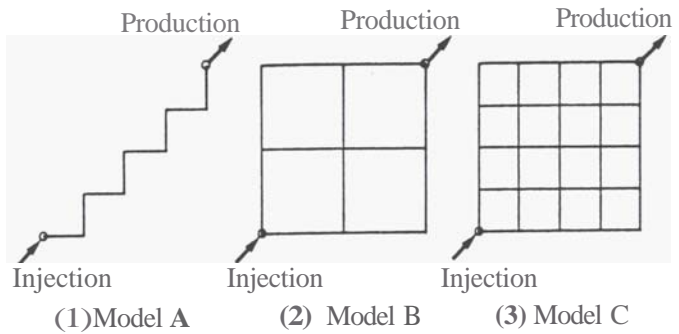


Figure 3- Idealized models of fracture flow path

3.1 The Effect of Water Injection Rate

Figs.4 and 5 show the performance of the bottom hole temperature of the production well and velocity distribution of the injected water through the fracture flow path B of Fig.3. The injection rate was varied as 2.5, 5.0 and 10.0 m³/day. Fig.4 indicates that as the injection rate increases, the bottom hole temperature decreases earlier and rapidly. This might be due to the following reasons: As shown in Fig.5, the velocity of the injected water in fracture flow path increases as the injection rate increases. Therefore the quantity of thermal energy transferred from the surrounding matrix rock to the injected water increases.

It could be said that the amounts of energy carried by the fluid flowing through fractures under the steady state

Table 1 Major Input Data for Sensitivity Studies

Injection/Production flow rate,	Q	=	1.25, 2.5, 5.0	$\text{m}^3/\text{day}/\text{m}$
Heat conductivity of matrix rock,	h ,	=	117, 201, 285	$\text{kJ}/\text{m} \cdot \text{day} \cdot ^\circ\text{C}$
Heat conductivity of water,	λ_1	=	58.6	$\text{kJ}/\text{m} \cdot \text{day} \cdot ^\circ\text{C}$
Specific heat capacity of matrix rock,	c_m	=	8.4	$\text{kJ}/\text{kg} \cdot ^\circ\text{C}$
Specific heat capacity of water,	c_f	=	4.2	$\text{kJ}/\text{kg} \cdot ^\circ\text{C}$
Matrix density,	ρ_m	=	2500	kg/m^3
Water density,	ρ_f	=	1000	kg/m^3
Initial temperature of matrix,	e_s	=	250	$^\circ\text{C}$
Initial temperature of fracture,	e_f	=	250	$^\circ\text{C}$
Injection water temperature,	θ_{in}	=	50	$^\circ\text{C}$

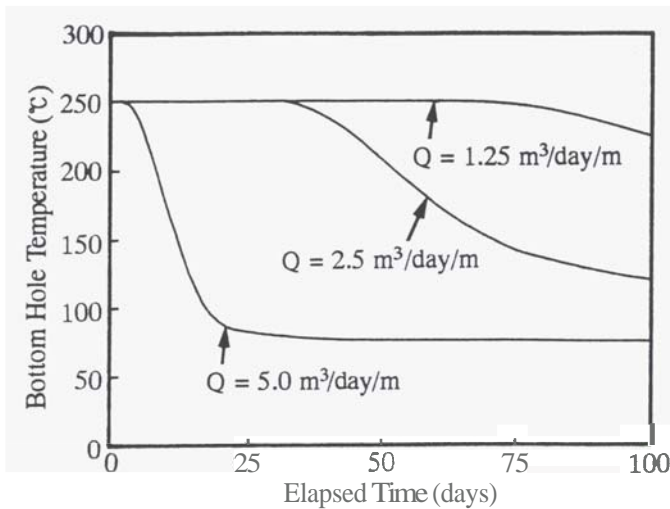
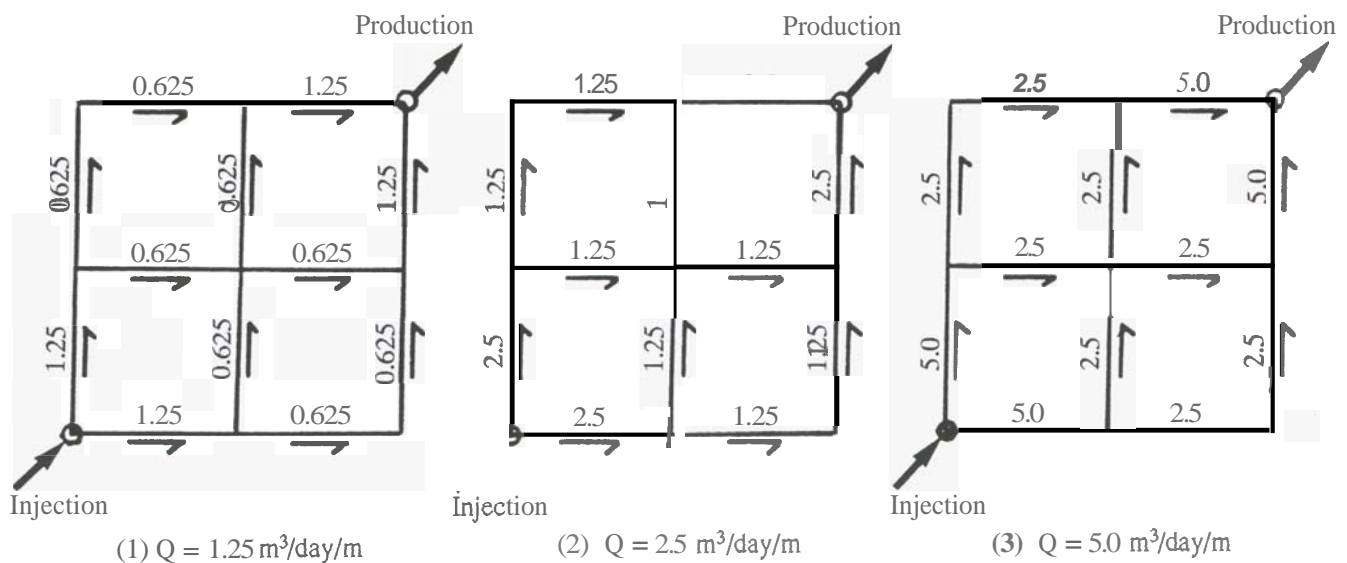


Figure 4- Sensitivity of bottom hole temperature to injection rate

condition almost equals to the enthalpy of the fluid before the injected water front reaches to the production well. That is, the enthalpy of the fluid is the main factor of the fluid temperature while the injected fluid is kept at high temperature. Afterwards, the fluid temperature begins to decrease and reaches to a certain level. This is because the difference between the amounts of energy conducted from matrix rock to the fracture fluid and the amounts carried by the fluid becomes gradually small and because the energy balance reaches its equilibrium state. This implies that the injection rate has a large influence on the bottom hole temperature of the production well.

3.2 The Effect of Thermal Conductivity of the Matrix Rock

Figd shows the performance of the bottom hole temperature



Unit of Velocity : m/day

Figure 5- Velocity distributions of injected water for different injection rates

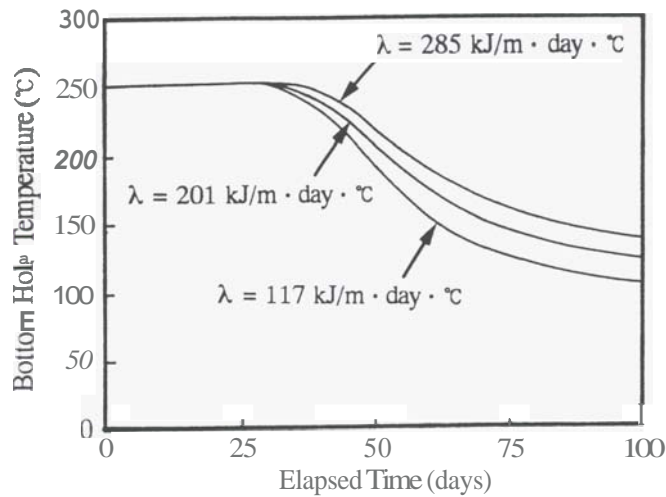


Figure 6- Sensitivity of bottom hole temperature to matrix rock thermal conductivity

of the production well when thermal conductivity of the matrix rock was varied as 28, 48 and 68 kcal/m · day · °C in the fracture flow path B of Fig.3. Fig.6 indicates that as the conductivity decreases, the bottom hole temperature tends to decrease rapidly. This is because the conductivity controls the amounts of energy supplied from matrix rock to the fluid flowing through fractures under the condition that temperature distributions in matrix rock of three kinds of different conductivity resemble each other.

3.3 The Effect of Drilling Mud Invasion

During the drilling of the production well, drilling mud breaks into fractures that are already existing in the matrix rock and makes the matrix rock cool down. Fig.7 shows the performance of the bottom hole temperature of the

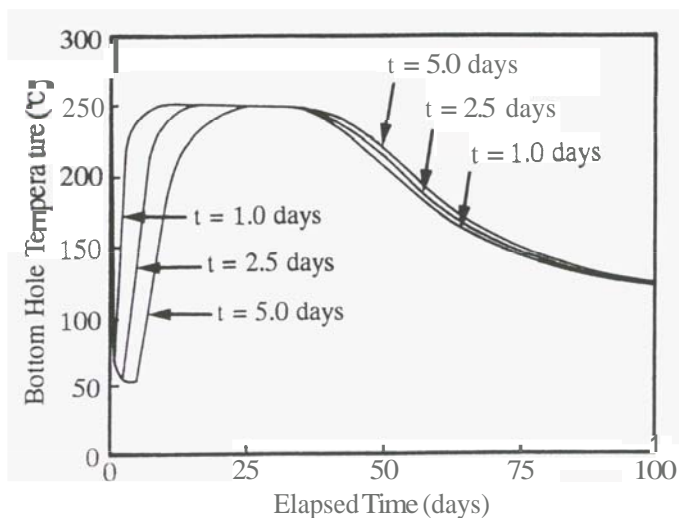


Figure 7- Sensitivity of bottom hole temperature to drilling mud duration time

production well when water was circulated from the injection well supposing that duration time, which is defined as the length of time drilling mud stayed in fractures in this paper, was varied 1.0, 2.5 and 5.0 days. The bottom hole temperature declines due to the stay of drilling mud and increases when the production starts. It takes longer to recover the bottom hole temperature up to 250°C, which is the initial temperature, as the duration time increases. After that, the bottom hole temperature begins to decrease at the almost same time without the influence of the duration time. These are due to that the matrix rock surrounding the fracture path was cooled down depending on the duration time.

This suggests that the length of hot water production time gets shorter influenced by the drilling mud which cool down the matrix rock while the production well is drilled.

3.4 The Effect of Connected Fracture Length

Fig.8 shows the performance of the bottom hole temperature of the production well for three different fracture flow path model A, B and C of Fig.3. For the calculations in this section, the duration time was set at 5 days. As the number of connected fractures increase, that is, fracture length improves, the bottom hole temperature tends to be kept high longer and then decreases gradually. This is because that each flow rate of fracture path reduces by splitting and heat exchange area between matrix rock and fractures increase in the case of large number of connected fracture paths and constant water injection rate as shown in Fig.9. This implies that heat extraction from artificial geothermal reservoir is more efficient in multiple fracture paths than in a single fracture path.

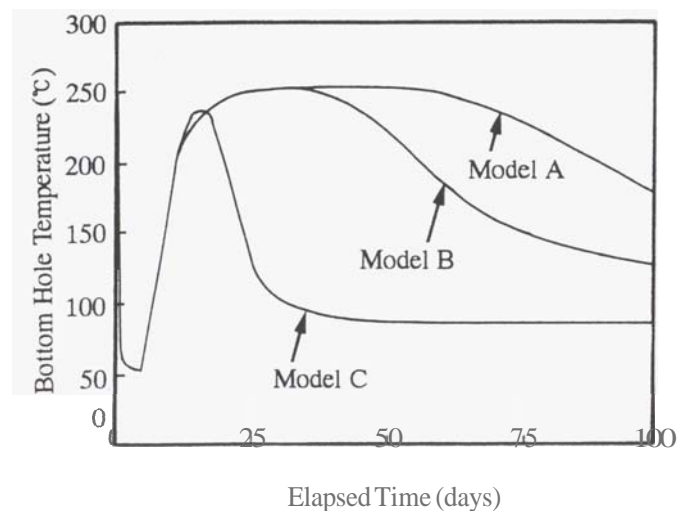


Figure 8- Sensitivity of bottom hole temperature to fracture flow path

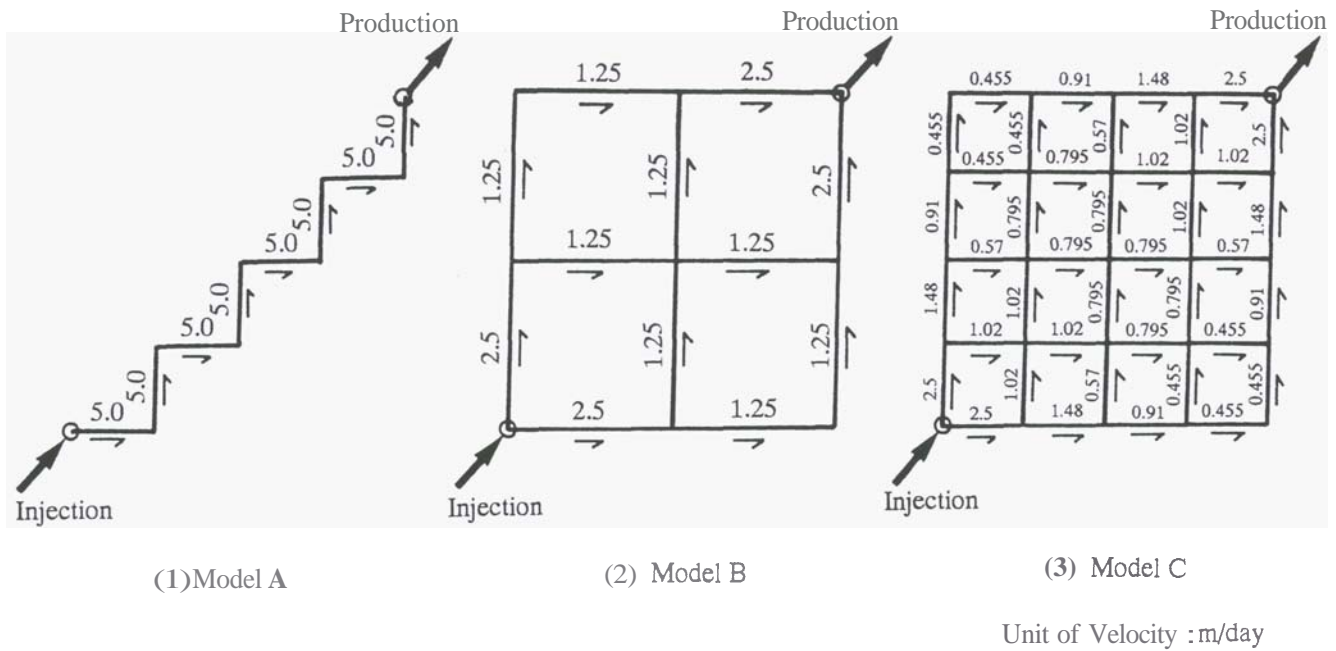


Figure 9- Velocity distributions of injected water for different flow paths

4. CONCLUSIONS

Following conclusions were obtained from sensitivity studies performed with the numerical model developed by the authors.

- 1) Water injection rate has a large influence on the bottom hole temperature of the production well.
- 2) Thermal conductivity of matrix rock controls the amounts of energy supplied from matrix rock to the fluid flowing through fractures.
- 3) The length of hot water production time gets shorter influenced by the drilling mud which cool down matrix rock while the production well is drilled.
- 4) Heat extraction from artificial geothermal reservoir is more efficient in multiple fracture paths than in a single fracture path.

5. ACKNOWLEDGEMENTS

The authors would like to acknowledge Mr. H. Kosukegawa for his co-operation in producing figures.

6. REFERENCES

- Akibayashi, S., Yamaguchi, S., M.Fukuda. (1992). A simulation model of heat extraction from hot dry rock. *Jnl. of the Geothermal Research Society of Japan*, Vol.14, No.3, 253-272.
- Chida, T. and Niibori, Y. (1990). Geothermal Reservoir Model, *Jnl. of the Mining and Material Processing Institute*

of Japan, Vol.106, N0.12, 705-712.

Gringarten, A.C., Witherspoon, P.A. and Ohnishi, Y. (1975). Theory of heat extraction from fractured hot dry rock, *Jnl. of Geophysical Research*, Vol.80, No.8, 1120-1124.

Kimura, S., Masuda, Y. and Hayashi, K. (1991). An efficient numerical method based on double porosity model to analyze heat and fluid flows in fractured rock formations, *Trans. of the Japan Society of Mechanical Engineers, (B)*-Vol.57, No.538, 157-161.

Masuda, Y., Kimura, S. and Hayashi, K. (1991). Heat extraction simulation from fractured rock by a double porosity and double permeability model, *Jnl. of the Geothermal Research Society of Japan*, Vol.13, No.3, 179-190.

NEDO, Geothermal Energy Department (1991). *Report on the status of geothermal energy research in Japan (1980-1989)*, Geothermal Resources Council BULLETIN, 103-111.

Pruess, K. and Narasimhan, T.N. (1985). A practical method for modeling fluid and heat flow in fractured porous media, *Soc. of Petroleum Engineers Journal*, February, 14-26.

Wkao, N., Kaguei, S. and Funaziri, T. (1979). Effect of fluid dispersion coefficients on particle-to-fluid heat transfer coefficients in packed beds, correlation of Nusselt numbers, *Chemical Engineering Science*, Vol.34, 325-36.